A NEW APPROACH TO THE THEORY OF LINEAR DICHROISM IN PARTIALLY ORDERED SYSTEMS

APPLICATION TO REACTION CENTERS AND WHOLE CELLS OF PHOTOSYNTHETIC BACTERIA

JOHN A. NAIRN, RICHARD FRIESNER, HARRY A. FRANK, AND KENNETH SAUER,
Department of Chemistry and Laboratory of Chemical Biodynamics, Lawrence Berkeley Laboratory, University of California, Berkeley, California 94720 U.S.A.

ABSTRACT We have developed a new approach to the theory of linear dichroism in partially ordered systems. The description of the partially ordered ensemble uses a density of states function, $D(\theta, \phi, \underset{\sim}{\Delta})$, which gives the probability that the direction of polarization for incident polarized light has spherical angles θ and ϕ in an axis system fixed with respect to the molecule; $\underset{\sim}{\Delta} = (\Delta_1, \Delta_2 \ldots \Delta_n)$ is a set of parameters that describes the partial ordering. We derive new formulas for linear dichroism using the density of states function and then apply these formulas to the analysis of linear dichroism in reaction centers and whole cells of photosynthetic bacteria. One advantage of our approach is that the order parameter, $\underset{\sim}{\Delta}$, provides a more complete description of the distribution function than the traditional order parameters used by other authors. Knowledge of $\underset{\sim}{\Delta}$ gives a good physical description of the partial ordering and allows one to calculate accurate limits for the range of possible orientations of the transition moments.

INTRODUCTION

Linear dichroism refers to a dependence of the absorption of polarized light on the direction of polarization. This dependence arises because the molecular absorbance due to a transition moment $\underset{\sim}{\mu}$ depends on the angle between $\underset{\sim}{\mu}$ and the polarized field $\underset{\sim}{E}$. An analysis of linear dichroism data can, therefore, enable one to extract structural information on the orientation of the transition moment. The theory is straightforward for single crystals or perfectly ordered systems (1, 2), but complex for partially ordered systems (2). We develop here a new approach to the theory of linear dichroism in partially ordered systems.

Most previous theories of linear dichroism in partially ordered systems have introduced an orientational distribution function $P(\theta', \phi', \psi')$ which gives the probability that a molecule-fixed axis system has Euler angles θ', ϕ', and ψ' with respect to the laboratory axis system (2) (Fig. 1). The distribution function can then be expanded in terms of the Wigner Rotation Matrices (3, 4)

$$P(\theta', \phi', \psi') = \sum_{l,m,n} P_{lmn}\, \mathcal{D}^{l}_{m,n}(\theta', \phi', \psi'), \tag{1}$$

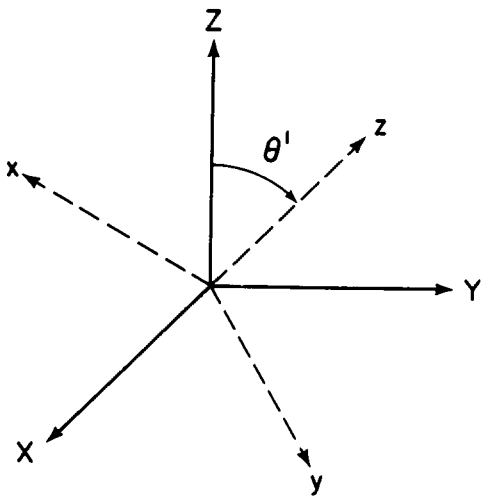

FIGURE 1

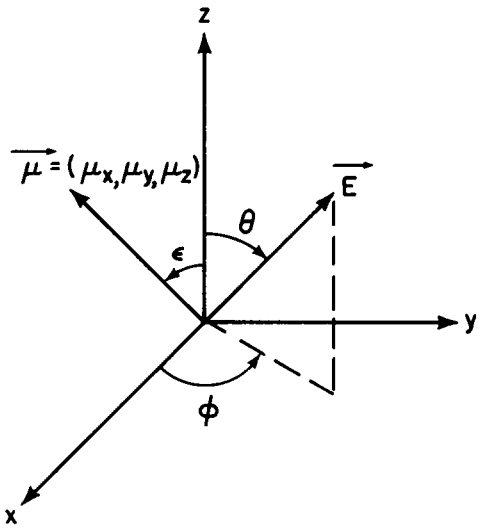

FIGURE 2

FIGURE 1 Relation between the laboratory axis system (labeled X,Y, and Z) and the molecular axis system, (labeled x, y, and z). θ' is one of the three Euler angles (θ', ϕ', and ψ') that relate the laboratory axis system to the molecular axis system.

FIGURE 2 Arrangement of $\underset{\sim}{\mu}$ and $\underset{\sim}{E}$ in the molecular axis system. θ and ϕ are the spherical angles of $\underset{\sim}{E}$.

where P_{lmn} is the lmnth moment of the distribution function defined by

$$P_{lmn} = \frac{2l+1}{8\pi^2} \int_0^{2\pi} \int_{-1}^{1} \int_0^{2\pi} P(\theta', \phi', \psi') \mathcal{D}^l_{m,n}(\theta', \phi', \psi') \, d\phi' \, d\cos\theta' \, d\psi'. \tag{2}$$

Use of Eq. 1 in traditional linear dichroism expressions yields equations which involve only the $l = 2$ moments (3). If the distribution function is axially symmetric, the resulting equations depend only on P_{200}, which is related to the traditionally used order parameter S (2) by $S = (1/3)(3 \langle \cos^2\theta' \rangle - 1) = (8\pi^2/5) P_{200}$, where $\langle \cos^2\theta' \rangle$ is the ensemble average of $\cos^2\theta'$ over the axially symmetric distribution function.

There are two basic problems with the Wigner expansion method. The first problem arises when one wants to use a linear dichroism experiment to find the orientation of $\underset{\sim}{\mu}$ in the molecular axis system. This determination requires knowledge of all of the $l = 2$ moments. The best way to approach this problem is to construct a model for the partially ordered system, calculate $P(\theta', \phi', \psi')$, and then calculate the $l = 2$ moments. However, no general method for calculation of $P(\theta', \phi', \psi')$ from a model has been described. The second problem arises when one knows the orientation of $\underset{\sim}{\mu}$ in the molecular axis system and hopes to use a linear dichroism experiment to learn something about the distribution function. At best, one can find the $l = 2$ moments, but these may be of little value in describing the distribution function if the Wigner expansion is slowly convergent.

Our approach to linear dichroism overcomes the above problems by using new techniques for describing partially ordered systems (5, 6) which we have already applied to simulation of

electron paramagnetic resonance (EPR) spectra (7). These techniques involve a general method for representing the distribution function in terms of a set of order parameters $\underset{\sim}{\Delta} = (\Delta_1, \Delta_2, \Delta_3, \ldots \Delta_n)$. We call the parametric representation of the distribution function, the density of states function, $D(\theta, \phi, \underset{\sim}{\Delta})$, and it gives the probability that the polarized field has spherical angles θ and ϕ in an axis system fixed with respect to the transition moment $\underset{\sim}{\mu}$ (Fig. 2). The chief difference between our approach and the Wigner expansion approach is that our $\underset{\sim}{\Delta}$ parameters are chosen from physical consideration of the partially ordered system, and as a result are likely to be fewer in number and more meaningful than the Wigner expansion moments. Note also that $D(\theta, \phi, \underset{\sim}{\Delta})$ is a distribution function in a molecular axis system, while $P(\theta', \phi', \psi')$ is a distribution function in the laboratory axis system. That is, we will be orientation averaging in a molecular axis system. As will be shown later, this approach leads to simplification of the formulas in many instances.

A brief summary of how to calculate a density of states function follows (for more details see references 5 and 6): (*a*) From a model for the system, one determines a set of rotations which rotate an axis system originally coincident with the laboratory axis system into an axis system which is a member of the ensemble of axis systems fixed with respect to the transition moment. (*b*) The rotations are assigned weighting functions giving the probability distribution in each rotation; e.g., a Gaussian weighted rotation about some axis will have the weighting function $\exp(-\beta^2/\Delta^2)$, where Δ is the width of the Gaussian. (*c*) Finally, $D(\theta, \phi, \underset{\sim}{\Delta})$ is obtained as an integral over the weighting functions (see Appendix A and references 5 and 6). The density of states function can then be used in linear dichroism expressions to yield equations which depend parametrically on the order parameter $\underset{\sim}{\Delta}$.

To determine the orientation of $\underset{\sim}{\mu}$ in the molecular axis system, one now needs to know $\underset{\sim}{\Delta}$ rather than the $l = 2$ moments. As stated above, the best approach is to construct a model, calculate $D(\theta, \phi, \underset{\sim}{\Delta})$, and interpret the linear dichroism. Because general methods exist for constructing $D(\theta, \phi, \underset{\sim}{\Delta})$ from a model, the density of states approach is more efficient than the Wigner expansion method. Furthermore, $D(\theta, \phi, \underset{\sim}{\Delta})$, unlike the $l = 2$ moments, can be used to interpret many types of experiments on a system, and the results often allow one to specify $\underset{\sim}{\Delta}$ within a small range (5–7). If all components of $\underset{\sim}{\Delta}$ can be found, a linear dichroism experiment will yield the orientation of $\underset{\sim}{\mu}$ in the molecular axis system. Unfortunately, $\underset{\sim}{\Delta}$ can rarely be specified with certainty; our analysis, then, allows one to use the uncertainty in $\underset{\sim}{\Delta}$ to place accurate limits on the orientation of the transition moment.

Our approach is again superior if one intends to use a known orientation of $\underset{\sim}{\mu}$ in the molecular axis system to learn something about the distribution function. In this case, a linear dichroism experiment may yield $\underset{\sim}{\Delta}$. In contrast to the $l = 2$ moments, the $\underset{\sim}{\Delta}$ parameter completely determines the distribution function. The $\underset{\sim}{\Delta}$ parameter also gives physical insight because it is generally related to some structural property of the ordered system.

The next section describes our approach to the theory of linear dichroism based on the density of states formalism. The new approach is then applied to reaction centers and whole cells of photosynthetic bacteria. In the discussion, we compare our approach with others in the literature (1–4, 8–13). We find that our approach is equivalent to the Wigner expansion method, but it has four distinct advantages. First, compared with parameters like the $l = 2$ moments, the set of parameters $\Delta_1, \Delta_2 \ldots \Delta_n$ are more intuitively descriptive of the system.

Second, $\underset{\sim}{\Delta}$ gives a complete definition of the distribution function. Third, it is straightforward to construct $D(\theta, \phi, \underset{\sim}{\Delta})$ from complex physical models and to interpret linear dichroism in light of these models. Fourth, by orientation averaging in a molecular axis system our approach is often much more efficient. For example, when neither the laboratory reference frame nor the molecular reference frame is axially symmetric, $P(\theta', \phi', \psi')$ depends on all three angles, because it takes three Euler angles to specify the orientation of one axis system with respect to another. In contrast, $D(\theta, \phi, \underset{\sim}{\Delta})$ specifies the spherical angles of the applied field, which is a vectorial quantity. Because it takes only two angles to specify the orientation of a vector, $D(\theta, \phi, \underset{\sim}{\Delta})$ never requires more than two angles. We can, therefore, analyze complex models with fewer angular variables.

THEORY

The dichroic ratio R of an absorption band is defined as the ratio of integrated absorption bands measured with light polarized parallel, $\underset{\sim}{E}_{\parallel}$, and perpendicular, $\underset{\sim}{E}_{\perp}$, to a given direction; i.e.,

$$R = A_{\parallel}/A_{\perp}, \tag{3}$$

where $A_{\parallel}$ and $A_{\perp}$ are the integrated absorbances. Most reported forms of linear dichroism can be related to R, as discussed in Appendix B. One notable exception is for experiments that directly measure $A_{\parallel} - A_{\perp}$ (14–16) and normalize by dividing by A_r, which is the absorbance of the corresponding randomly oriented sample. We call this form the dichroic polarization, defined as:

$$L = \frac{A_{\parallel} - A_{\perp}}{A_r} \tag{4}$$

When the laboratory reference frame is axially symmetric, L can be related to R, but in the general nonaxially symmetric case L cannot be related to R. Therefore, we also derive formulas for L.

Before continuing, let us formally define the two coordinate systems which we have already mentioned. The first coordinate system is the laboratory axis system (XYZ), and it is fixed in the laboratory reference frame. In the laboratory axis system $\underset{\sim}{E}_{\parallel}$ and $\underset{\sim}{E}_{\perp}$ are constant vectors. The second coordinate system is the molecular axis system (xyz), and it is fixed with respect to the transition moment whose linear dichroism is being measured; that is, a unit vector $\hat{\mu}$ in the direction of the transition moment $\underset{\sim}{\mu}$ is a constant vector

$$\hat{\mu} = (\mu_x, \mu_y, \mu_z) \tag{5}$$

in the molecular axis system. In general, the set of molecular axis systems defines a partially ordered ensemble. We have previously discussed a method for direct determination of the density of states functions $D_{\parallel}(\theta, \phi, \underset{\sim}{\Delta})$ and $D_{\perp}(\theta, \phi, \underset{\sim}{\Delta})$ (5, 6). These functions give the probability that $\underset{\sim}{E}_{\parallel}$ and $\underset{\sim}{E}_{\perp}$ have spherical angles θ and ϕ in the molecular axis system; i.e., the probability that

$$\underset{\sim}{E} = |\underset{\sim}{E}|(\sin\theta\cos\phi, \sin\theta\sin\phi, \cos\theta). \tag{6}$$

Using the density of states formalism, we can now develop a new approach to the theory of linear dichroism.

We begin by calculating $A_\parallel$. The absorbance of a transition moment $\underset{\sim}{\mu}$ interacting with a polarized field $\underset{\sim}{E}$ is proportional to $(\underset{\sim}{\mu} \cdot \underset{\sim}{E})^2$ or, equivalently, to $\cos^2\beta$, where β is the angle between $\underset{\sim}{\mu}$ and $\underset{\sim}{E}$. For a partially ordered ensemble interacting with $\underset{\sim}{E}_\parallel$, the absorbance is

$$A_\parallel = K \int_0^\pi d\theta \int_0^{2\pi} d\phi (\hat{\mu} \cdot \underset{\sim}{E})^2 D_\parallel(\theta, \phi, \underset{\sim}{\Delta}) / \int_0^\pi d\theta \int_0^{2\pi} d\phi D_\parallel(\theta, \phi, \underset{\sim}{\Delta}), \tag{7}$$

where $\hat{\mu}$ and $\underset{\sim}{E}$ are defined by Eqs. 5 and 6, and K is an experimental constant which contains such parameters as extinction coefficient, concentration, and path length. (Note that in Eq. 7 and throughout this paper we use unnormalized density of states functions; the denominator furnishes the required normalization). Experimentally, the partial ordering is induced by exerting some type of force on the system, such as an alignment field or a mechanical stretch. Because the sign of the direction of these forces is arbitrary, the density of states has the following symmetry properties:

(1) $$D_\parallel(\theta, \phi, \underset{\sim}{\Delta}) = D_\parallel(\theta, \phi + \pi, \underset{\sim}{\Delta}), \tag{8}$$

and

(2) $$D_\parallel(\theta, \phi, \underset{\sim}{\Delta}) = D_\parallel(\pi - \theta, \phi, \underset{\sim}{\Delta}), \tag{9a}$$

$$D_\parallel(\theta, \phi, \underset{\sim}{\Delta}) = D_\parallel(\theta, \pi - \phi, \underset{\sim}{\Delta}). \tag{9b}$$

That is, $D_\parallel(\theta, \phi, \underset{\sim}{\Delta})$ is periodic with period π and is symmetric about $\pi/2$. Using only these symmetry properties, Eq. 7 reduces to

$$A_\parallel = K' \{\mu_x^2 [T_\parallel(\underset{\sim}{\Delta}) - F_\parallel(\underset{\sim}{\Delta})] + \mu_y^2 F_\parallel(\underset{\sim}{\Delta}) + \mu_z^2 [1 - T_\parallel(\underset{\sim}{\Delta})]\}, \tag{10}$$

where K' is a new constant,

$$T_\parallel(\underset{\sim}{\Delta}) = \int_0^{\pi/2} d\theta \sin^2\theta \int_0^{\pi/2} d\phi D_\parallel(\theta, \phi, \underset{\sim}{\Delta}) / N_\parallel(\underset{\sim}{\Delta}), \tag{11}$$

$$F_\parallel(\underset{\sim}{\Delta}) = \int_0^{\pi/2} d\theta \sin^2\theta \int_0^{\pi/2} d\phi \sin^2\phi D_\parallel(\theta, \phi, \underset{\sim}{\Delta}) / N_\parallel(\underset{\sim}{\Delta}), \tag{12}$$

and

$$N_\parallel(\underset{\sim}{\Delta}) = \int_0^{\pi/2} d\theta \int_0^{\pi/2} D_\parallel(\theta, \phi, \underset{\sim}{\Delta}). \tag{13}$$

In a random sample, $A_\parallel = A_r$, $D_\parallel(\theta, \phi, \underset{\sim}{\Delta}) = \sin\theta$, $T_\parallel(\underset{\sim}{\Delta}) = \frac{2}{3}$, and $F_\parallel(\underset{\sim}{\Delta}) = \frac{1}{3}$. Using these facts, we find that $K' = 3A_r$, and Eq. 10 for the ordered sample becomes

$$A_\parallel = 3A_r \{\mu_x^2 [T_\parallel(\underset{\sim}{\Delta}) - F_\parallel(\underset{\sim}{\Delta})] + \mu_y^2 F_\parallel(\underset{\sim}{\Delta}) + \mu_z^2 [1 - T_\parallel(\underset{\sim}{\Delta})]\}. \tag{14}$$

An analogous expression holds for $A_\perp$, where we define $T_\perp(\underset{\sim}{\Delta})$, $F_\perp(\underset{\sim}{\Delta})$, and $N_\perp(\underset{\sim}{\Delta})$ using $D_\perp(\theta, \phi, \underset{\sim}{\Delta})$. The dichroic ratio is thus given by

$$R = \frac{A_\parallel}{A_\perp} = \frac{\mu_x^2 [T_\parallel(\underset{\sim}{\Delta}) - F_\parallel(\underset{\sim}{\Delta})] + \mu_y^2 F_\parallel(\underset{\sim}{\Delta}) + \mu_z^2 [1 - T_\parallel(\underset{\sim}{\Delta})]}{\mu_x^2 [T_\perp(\underset{\sim}{\Delta}) - F_\perp(\underset{\sim}{\Delta})] + \mu_y^2 F_\perp(\underset{\sim}{\Delta}) + \mu_z^2 [1 - T_\perp(\underset{\sim}{\Delta})]} \tag{15}$$

and the dichroic polarization is given by

$$L = \frac{A_\parallel - A_\perp}{A_r} = 3\{\mu_x^2[T_\parallel(\underset{\sim}{\Delta}) - T_\perp(\underset{\sim}{\Delta}) + F_\perp(\underset{\sim}{\Delta}) - F_\parallel(\underset{\sim}{\Delta})] + \mu_y^2[F_\parallel(\underset{\sim}{\Delta}) - F_\perp(\underset{\sim}{\Delta})] + \mu_z^2[T_\perp(\underset{\sim}{\Delta}) - T_\parallel(\underset{\sim}{\Delta})]\}. \quad (16)$$

Eqs. 15 and 16 take simpler forms when the density of states depends only on θ and $\underset{\sim}{\Delta}$, which happens whenever the molecular reference frame is axially symmetric. Eqs. 11 and 12 become

$$T_\parallel(\underset{\sim}{\Delta}) = \int_0^{\pi/2} \sin^2\theta D_\parallel(\theta, \underset{\sim}{\Delta})\, d\theta \Big/ \int_0^{\pi/2} D_\parallel(\theta, \underset{\sim}{\Delta})\, d\theta \quad (17)$$

and

$$F_\parallel(\underset{\sim}{\Delta}) = \tfrac{1}{2}T_\parallel(\underset{\sim}{\Delta}). \quad (18)$$

The dichroic ratio reduces to

$$R = \frac{T_\parallel(\underset{\sim}{\Delta}) + \mu_z^2[2 - 3T_\parallel(\underset{\sim}{\Delta})]}{T_\perp(\underset{\sim}{\Delta}) + \mu_z^2[2 - 3T_\perp(\underset{\sim}{\Delta})]} \quad (19)$$

If the laboratory reference frame is also axially symmetric and $\underset{\sim}{E}_\parallel$ is along the symmetry axis,

$$A_r = \tfrac{1}{3}(A_\parallel + 2A_\perp). \quad (20)$$

When Eq. 20 holds, we can relate $T_\parallel(\underset{\sim}{\Delta})$ to $T_\perp(\underset{\sim}{\Delta})$; that relation is

$$T_\perp(\underset{\sim}{\Delta}) = 1 - \tfrac{1}{2}T_\parallel(\underset{\sim}{\Delta}). \quad (21)$$

Furthermore

$$L = \frac{3(A_\parallel - A_\perp)}{A_\parallel + 2A_\perp} \quad (22)$$

L in this form is related to R, as shown in Appendix B. If $\underset{\sim}{E}_\parallel$ is not along a laboratory symmetry axis, Eq. 20 is no longer valid, but we can still write

$$L = \tfrac{3}{2}\{[T_\perp(\underset{\sim}{\Delta}) - T_\parallel(\underset{\sim}{\Delta})](3\mu_z^2 - 1)\}. \quad (23)$$

We choose the z axis to be the axis of symmetry in the molecular axis system. The angle between the z axis and the transition moment $\underset{\sim}{\mu}$ is (Fig. 2)

$$\epsilon = \cos^{-1}\mu_z. \quad (24)$$

From Eq. 19

$$\epsilon = \cos^{-1}\left[\frac{1}{3 + \dfrac{2(1 - R)}{RT_\perp(\underset{\sim}{\Delta}) - T_\parallel(\underset{\sim}{\Delta})}}\right]^{1/2} \quad (25)$$

We now consider some special cases of Eq. 19. One type of perfect ordering is where all molecular z axes line up with the laboratory Z axis. If linear dichroism is measured with $\underline{E}_\parallel = (0, 0, 1)$ and $\underline{E}_\perp = (1, 0, 0)$, we have $D_\parallel(\theta) = \delta(\theta)$, $D_\perp(\theta) = \delta[(\pi/2) - \theta]$, $T_\parallel(\underline{\Delta}) = 0$, and $T_\perp(\underline{\Delta}) = 1$, where δ is a Dirac delta function.

Substitution into Eq. 19 gives the result first derived by Fraser (8):

$$R = 2\cot^2\epsilon. \tag{26}$$

The opposite extreme is a random sample, where $D_\parallel(\theta) = D_\perp(\theta) = \sin\theta$ and $T_\parallel = T_\perp = 2/3$. The dichroic ratio is $R = 1$; i.e., there is no linear dichroism. In the general partially ordered case, a calculation of $T_\parallel(\underline{\Delta})$ and $T_\perp(\underline{\Delta})$ is sufficient to interpret the linear dichroism.

In the next section, we will apply these formulas to some examples. Most reports of dichroic ratios are ratios of the peak absorbances rather than the integrated absorbances. As long as the parallel and perpendicular lineshapes do not differ too much, the ratio of peak absorbances is a close approximation to the "true" dichroic ratio. We will therefore ignore this difficulty. Another difficulty arises from band overlap of several transitions. When band overlap occurs, it is difficult to measure the dichroic ratio by measuring peak absorbances. We will attempt to analyze only pure transitions and hence avoid this problem.

RESULTS

The procedure for analyzing linear dichroism is the same for all systems. First, from a characterization of the absorption spectrum, one decides which bands are pure enough for an analysis. Second, from a consideration of the symmetry properties of the system, one calculates the parallel and perpendicular density of states, $D_\parallel(\theta, \phi, \underline{\Delta})$ and $D_\perp(\theta, \phi, \underline{\Delta})$. Last, the formulas in the last section are used to extract all of the possible structural information. We begin by analyzing the linear dichroism for a common experimental situation.

Gaussian Uniaxial Model

A common situation in which the molecular reference frame is axially symmetric is when the symmetry axis tends to align along the direction of an applied force (e.g., magnetic field direction or stretch direction). If we take the applied force to be along the laboratory Z axis, then deviations from perfect order are manifested by a nonzero angle β, between the symmetry axis and the laboratory Z axis. A partially ordered ensemble will be described by a probability distribution in β. In the Gaussian Uniaxial Model, we take the distribution to be a Gaussian of width Δ_G

$$w_G = w(\beta) = \exp(-\beta^2/\Delta_G^2). \tag{27}$$

(Note: Throughout this paper it is understood that our weighting functions are defined on the interval -90 to $90°$ and extended beyond this interval by symmetry; i.e., the weighting functions are periodic with a period of $180°$ and symmetric about $90°$.) This situation is illustrated in Fig. 3 a; each symmetry axis that points along the cone of half angle β about the laboratory Z axis will have the same probability of occurrence.

We seek a set of n rotations $R_1(\alpha_1)$, $R_2(\alpha_2)$, . . . $R_n(\alpha_n)$ and a weighting function $w(\alpha_1, \alpha_2, \ldots \alpha_n)$ that will generate the ensemble in the Gaussian Uniaxial Model. That is, a weighting function which describes the probability that the molecular axis system for a member of the

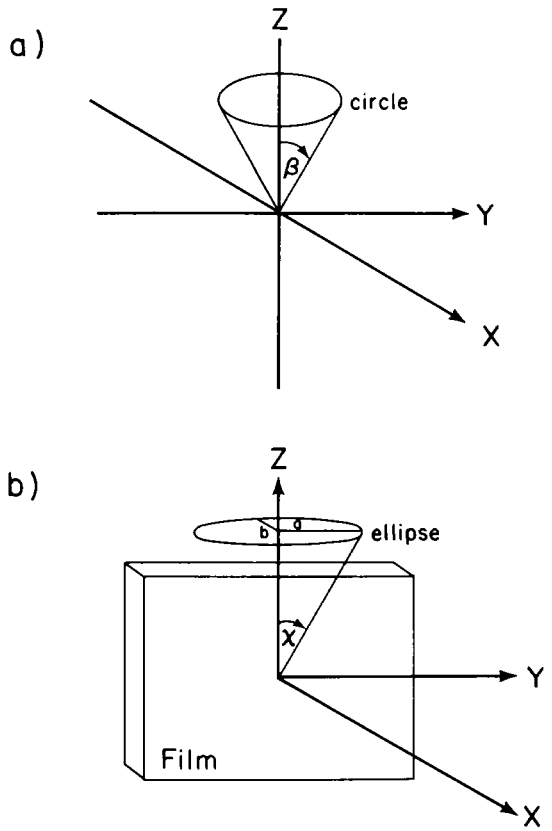

FIGURE 3 (*a*) Schematic representation of the Gaussian Uniaxial Model. β is the half-angle of the cone centered on the laboratory Z axis. (*b*) Schematic representation of the Elliptical Gaussian Uniaxial Model. χ is the angle between the laboratory Z axis and the line in the YZ plane that points to the ellipse. a and b are the major and minor axes of the ellipse.

ensemble is related to the laboratory axis system by n rotations of $\alpha_1, \alpha_2 \ldots \alpha_n$, respectively. The ensemble in the Gaussian Uniaxial Model can be generated by the following three-rotation scheme: a free rotation of α about the laboratory Z axis (by free rotation, we mean the weighting function does not depend on α); a Gaussian weighted rotation of β about the laboratory Y axis; a free rotation of γ of about the laboratory Z axis. The weighting function for these three rotations is given by Eq. 27. As discussed in references 5 and 6, (see Appendix A), the density of states is easy to calculate given w_G, $\underset{\sim}{E}_\parallel$, and $\underset{\sim}{E}_\perp$. Typically, $\underset{\sim}{E}_\parallel$ is along the laboratory Z axis and $\underset{\sim}{E}_\perp$ is along the laboratory X axis (or any axis in the XY plane), which means $D_\parallel(\theta, \Delta_G)$ and $D_\perp(\theta, \Delta_G)$ are (in the notation of reference 6; see Appendix A)

$$D_\parallel(\theta, \Delta_G) = D^{ZYZ}_{3,90}[\theta, w_G] \tag{28}$$

and

$$D_\perp(\theta, \Delta_G) = D^{ZYZ}_{1,0}[\theta, w_G]. \tag{29}$$

$D_\parallel(\theta, \Delta_G)$, $D_\perp(\theta, \Delta_G)$, $T_\parallel(\Delta_G)$ and $T_\perp(\Delta_G)$ are plotted in Fig. 4 for several values of Δ_G.

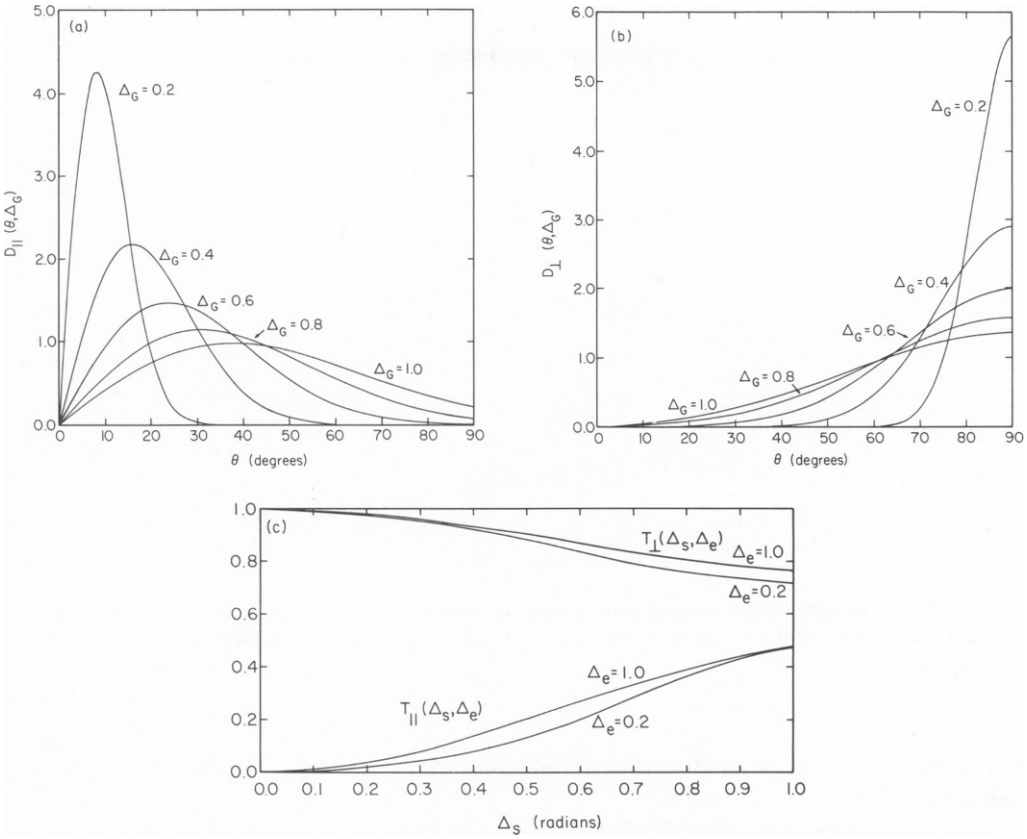

FIGURE 4 (*a*) $D_{||}(\theta, \Delta_G)$ for the Gaussian Uniaxial Model for several values of Δ_G in radians. (*b*) $D_{\perp}(\theta, \Delta_G)$ for the Gaussian Uniaxial Model for several values of Δ_G in radians. (*c*) $T_{||}(\Delta_G)$ and $T_{\perp}(\Delta_G)$ for the Gaussian Uniaxial Model ($\Delta_e = 1.0$) and for the Elliptical Gaussian Uniaxial Model with $\Delta_e = 0.2$.

In Fig. 5, we plot the dichroic ratio, R, as calculated from Eq. 19, versus the angle between the symmetry axis of the particle and the transition moment. Note that perfect ordering, $\Delta_G = 0.0$, corresponds to $R = 2\cot^2\epsilon$, as shown in the Theory section. For perfect ordering, R can assume any positive number; but, as Δ_G increases, R becomes bounded on both sides. This fact can often be useful in determining an upper limit for Δ_G. In Fig. 6, we plot ϵ versus Δ_G for various values of R. If $R < 1$, ϵ ranges from the perfect order value derived from Eq. 26 to 90° and, if $R > 1$, ϵ ranges from the perfect order value to 0°. Fig. 6 allows one again to infer limits on Δ_G, given a measurement of R, because ϵ cannot fall outside the range 0 to 90°.

Rhodopseudomonas sphaeroides in Stretched Films

Two recent papers by Rafferty and Clayton (17, 18) describe the linear dichroism spectra of reaction centers of *Rps. sphaeroides* in both stretched and unstretched films. The reaction center particles contain four bacteriochlorophyll *a* (BChl *a*) molecules and two bacteriopheophytin a (BPh *a*) molecules, which all contribute to a complicated absorption spectrum (19). We choose to study the 860-nm transition because it is believed to be a pure transition of

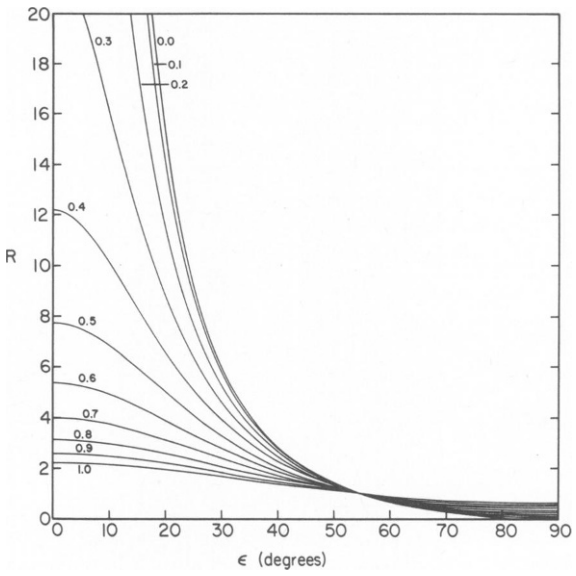

FIGURE 5 Dichroic ratio R versus angle ϵ between the transition moment μ and the symmetry axis of the molecular reference frame. The plots are for the Gaussian Uniaxial Model with several values of Δ_G in radians.

P860, which is a BChl *a* dimer that functions as the primary electron donor in *Rps. sphaeroides* (20).

We assume, as did Rafferty and Clayton (17, 18), that the reaction center particles possess an axis of symmetry which tends to align with the stretch direction. As a first approximation, this assumption is isomorphic to the Gaussian Uniaxial Model; we take the width of the Gaussian distribution of particle orientations within their stretched film to be Δ_S.

At 860 nm, Rafferty and Clayton (17, 18) measure $R = 2.28$, which means $\epsilon < 43°$. Furthermore, $\Delta_S \leq 1.0$ rad (see $\Delta_G = 1.0$ curve in Fig. 5). We can narrow the limits on Δ_S further by considering the value of R at a different wavelength. At 597 nm, they measure $R = 0.48$. If we assume this to be a pure transition, we have a new limit: $\Delta_S \leq 0.75$ rad. In reality, the 597-nm transition is not a pure transition, but this means that the 597-nm linear dichroism must contain at least one component whose R value is not greater than 0.48. Therefore, the limit of 0.75 rad on Δ_S is an upper limit because it is based on the conservative assumption that the 597-nm transition is a pure transition. Rafferty and Clayton (17, 18) did experiments on films that were stretched to different extents. At 860 nm in one such film, they determined R to be as high as 2.50. An R of 2.50 means that ϵ must be $\leq 42°$. Returning to the film where $R = 2.28$, we find that imposing the restriction of $\epsilon \leq 42°$ requires that Δ_S must be ≤ 0.30 rad. The final, most conservative, limits on Δ_S are

$$0.30 \text{ rad} \leq \Delta_S \leq 0.75 \text{ rad}. \tag{30}$$

From Eq. 25, the limits of ϵ are

$$29° \leq \epsilon \leq 42°. \tag{31}$$

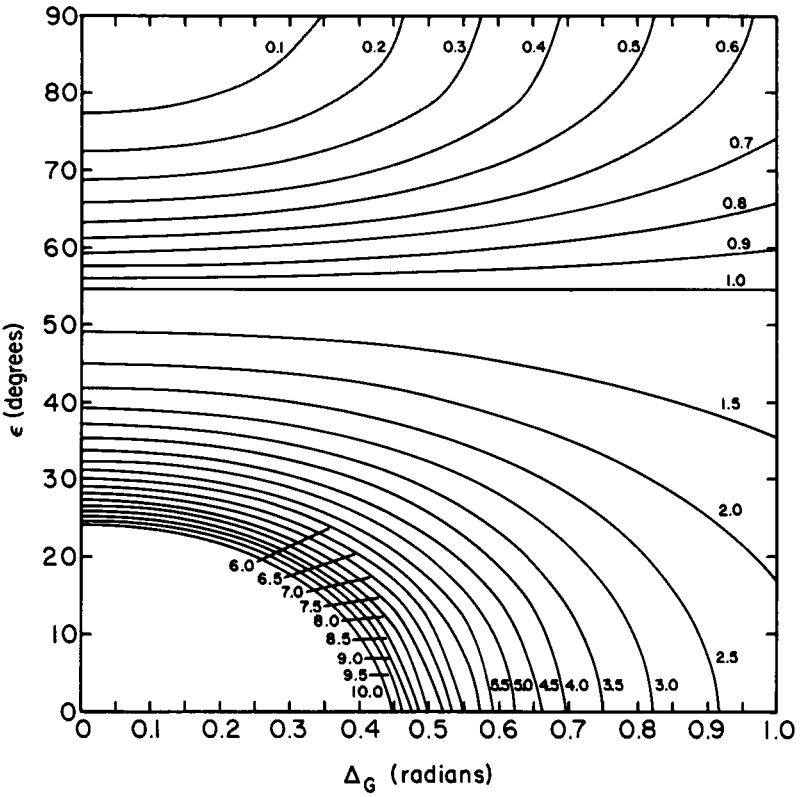

FIGURE 6 Angle ϵ between the transition moment μ and the symmetry axis of the molecular reference frame versus Δ_G in radians. The plots are for the Gaussian Uniaxial Model with several values of the dichroic ratio R.

Perhaps the Gaussian Uniaxial Model is an oversimplification, because it neglects the anisotropy of the unstretched film; i.e., it neglects the possibility that the particle symmetry axes lie in the plane of the unstretched film. We will therefore consider a more sophisticated model. Instead of giving equal weights to all symmetry axes that lie on the circle in Fig. 3 *a*, we can use the model illustrated in Fig. 3 *b*, where all symmetry axes that lie on an ellipse have equal weights. Upon stretching, it is more likely that the tilt of the particle symmetry axis away from the laboratory Z axis is in, rather than out of, the plane of the film. Therefore, the ratio of the ellipse axes $\Delta_e = b/a$ is <1. We call this model the Elliptical Gaussian Uniaxial Model; it can be generated by the same rotations as the Gaussian Uniaxial Model, but the product of the weighting functions is now

$$w_{EG} = w(\beta, \gamma) = \exp(-\chi^2/\Delta_S^2), \tag{32}$$

where

$$\chi = \tan^{-1}\left[\tan\beta\left(\frac{\sin^2\gamma}{\Delta_e^2} + \cos^2\gamma\right)^{1/2}\right]. \tag{33}$$

Despite the loss of axial symmetry in the laboratory reference frame, $D_{\parallel}(\theta, \Delta_S, \Delta_e)$ and

$D_\perp(\theta, \Delta_S, \Delta_\epsilon)$ are still axially symmetric. In the Wigner expansion method, axial symmetry would be lost and the analysis would become much more complicated.

$T_\parallel(\Delta_S, \Delta_\epsilon)$ and $T_\perp(\Delta_S, \Delta_\epsilon)$ for $\Delta_\epsilon = 1.0$ (Gaussian Uniaxial Model) and $\Delta_\epsilon = 0.2$ are plotted in Fig. 4 *c*. We can pick a trial value for Δ_ϵ and analyze the linear dichroism data just as we did with the Gaussian Uniaxial Model. We find that the limits on ϵ in Eq. 31 are independent of Δ_ϵ, and thus Eq. 31 is consistent with the Elliptical Gaussian Uniaxial Model.

Rafferty and Clayton (17, 18) calculated ϵ to be 40.8° by assuming that an extrapolated value of $R = 2.68$ at 860 nm corresponds to perfect order. This value falls within our limits but, if the extrapolation is invalid, the range of ϵ in Eq. 31 provides a more realistic interpretation of their data. The question can be resolved by using $D_\parallel(\theta, \Delta_S)$ and $D_\perp(\theta, \Delta_S)$ to analyze other types of experiments and thereby pin down Δ_S.

Rps. sphaeroides in Unstretched Films

Rafferty and Clayton (17, 18) also did some linear dichroism experiments on unstretched film containing reaction center particles of *Rps. sphaeroides*. We use a model similar to Rafferty and Clayton's (17, 18) which assumes that the reaction center particle symmetry axis lies close to the plane of the film. However, the film is not perfectly ordered; some of the symmetry axes are not in the plane of the film but are tilted out of the film by an angle β. The partial ordering is thus described by a probability distribution in β for which we use a Gaussian

$$w_{US} = w(\beta) = \exp(-\beta^2/\Delta_{US}^2), \tag{37}$$

where Δ_{US} is the width of the Gaussian distribution.

The Gaussian Uniaxial Model is not appropriate here. But, using the coordinate system shown in Fig. 3 *b*, this ensemble can be generated with the following three-rotation scheme: a free rotation of α about the laboratory Z axis; a Gaussian weighted rotation of β about the

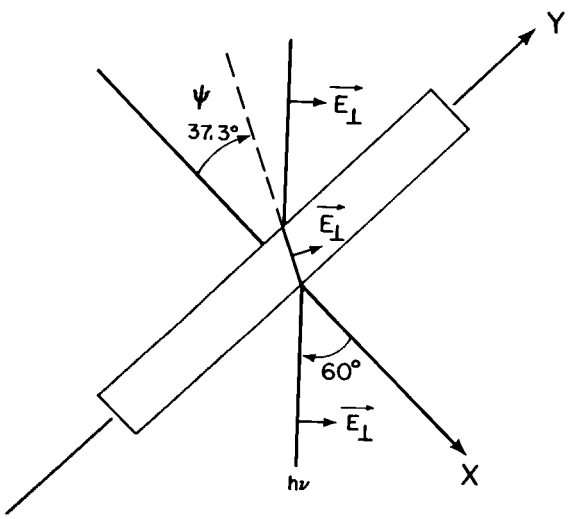

FIGURE 7 Propagation of $\underline{E}_\perp$ through unstretched films as in the experimental set up of Rafferty and Clayton (17, 18).

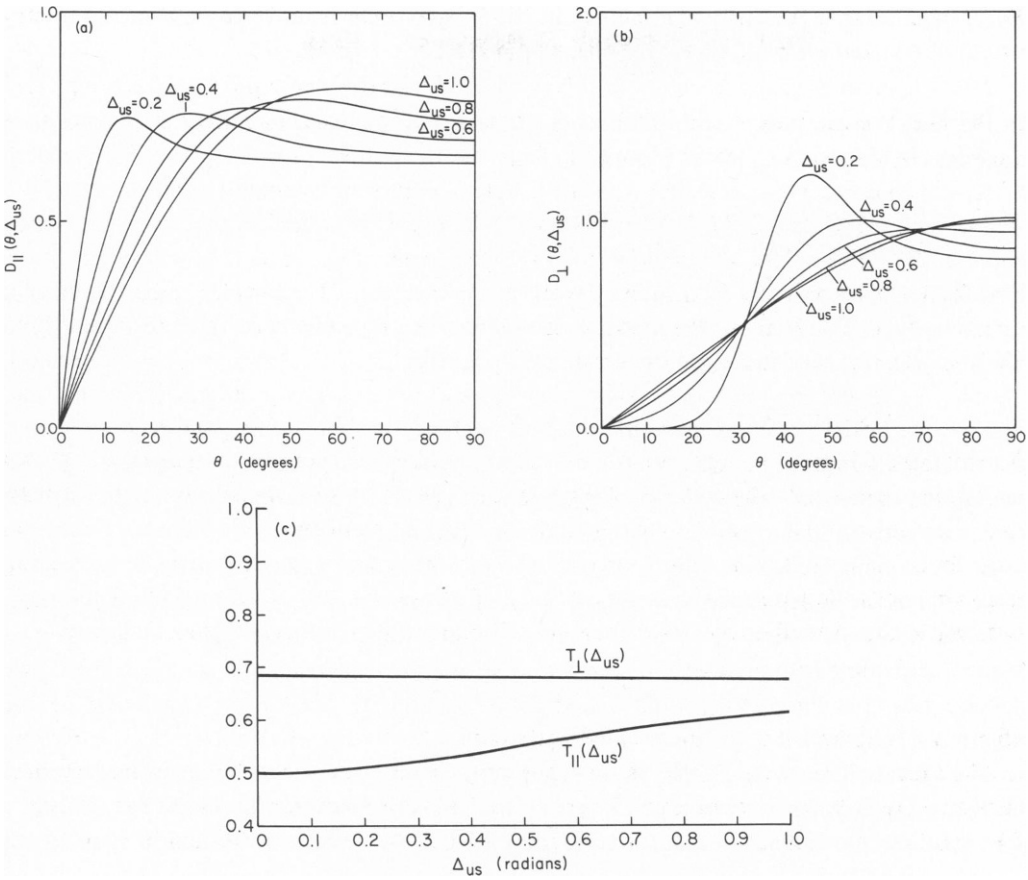

FIGURE 8 (*a*) $D_{\|}(\theta, \Delta_{US})$ for unstretched films for several values of Δ_{US} in radians. (*b*) $D_{\perp}(\theta, \Delta_{US})$ for unstretched films for several values of Δ_{US} in radians. (*c*) $T_{\|}(\Delta_{US})$ and $T_{\perp}(\Delta_{US})$ for unstretched films.

laboratory Y axis; and a free rotation of γ about the laboratory X axis. The product of the weighting functions for these rotations is given by Eq. 37.

To observe linear dichroism in unstretched films, the experiment must be done with a light propagation direction that is not normal to the plane of the film. Fig. 7 shows the geometry employed by Rafferty and Clayton (17, 18). Within the boundaries of the film, $\underline{E}_{\|} = (0, 0, 1)$ and $\underline{E}_{\perp} = (\sin\psi, \cos\psi, 0)$, where $\psi = 37.3°$. In the notation of reference 6,

$$D_{\|}(\theta, \Delta_{US}) = D^{ZYX}_{3,90}[\theta, w_{US}], \tag{38}$$

and

$$D_{\perp}(\theta, \Delta_{US}) = D^{ZYX}_{1,52.7}[\theta, w_{US}]. \tag{39}$$

$D_{\|}(\theta, \Delta_{US})$, $D_{\perp}(\theta, \Delta_{US})$, $T_{\|}(\Delta_{US})$, and $T_{\perp}(\Delta_{US})$ are plotted for several values of Δ_{US} in Fig. 8.

From the range of ϵ given in Eq. 31, we can determine a range for Δ_{US}; that is, a linear dichroism analysis will tell us how well the reaction center particles orient in unstretched films. Rafferty and Clayton (17, 18) measured a dichroic ratio of $R = 1.14$ at 860 nm. From

Eq. 19 we find that the width of the Gaussian distribution in β is restricted to the range

$$0.45 \text{ rad} \leq \Delta_{US} \leq 0.90 \text{ rad}. \tag{40}$$

In the next two sections, we consider some additional systems where experiments have been done that determine $\underset{\sim}{\Delta}$ to within a small range.

Rhodopseudomonas viridis and Rhodopseudomonas palustris in a Magnetic Field: the Density of States

Both *Rps. viridis* cells and *Rps. palustris* cells are cylindrical (21, 22), and can be aligned in a magnetic field such that the long axis of the cylinder is perpendicular to the alignment field (23). Inside the cells are cylindrical membrane shells (21, 22) containing bound chromophores. We choose the molecular axis system to have its z axis along the membrane normal. We select a model which assumes that the chromophores are bound in a fixed relation to, and distributed around, the membrane normal, an assumption consistent with experiments. In this model, the molecular reference frame is axially symmetric. Furthermore, the angle ϵ will be the angle between the membrane normal and the transition moment.

In this system, we cannot use the Gaussian Uniaxial Model as an approximation, because the z axis of the molecular axis system does not align preferentially along the magnetic field. It is the whole cells that are oriented by the magnetic field; the ensemble of molecular axis systems distributed throughout the membranes is oriented as a consequence. As a model, we assume that the long axis of the cylinder representing the cell is perpendicular to the alignment field and that deviations from perfect order are due to deviations of the membranes from perfect cylinders. The angle between the actual membrane normal and the hypothetical perfect cylinder normal is assumed to have a Gaussian distribution with width Δ_C. ($\Delta_C = \Delta_{RV}$ for *Rps. viridis* and Δ_P for *Rps. palustris*.) Calculation of $D_{\parallel}(\theta, \Delta_C)$ and $D_{\perp}(\theta, \Delta_C)$ is

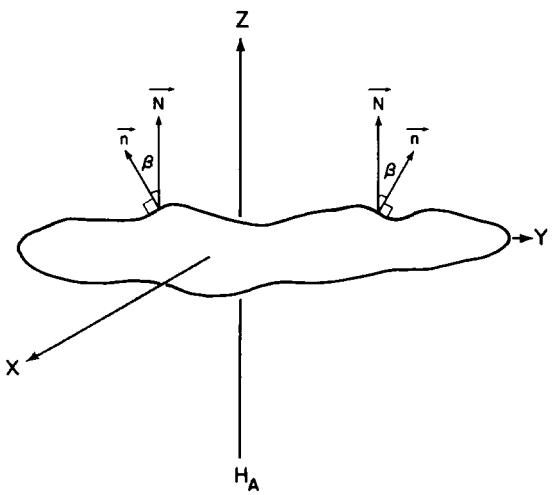

FIGURE 9 Definition of the angles and axis systems for *Rps. viridis* and *Rps. palustris* in a magnetic field. The alignment field $\underset{\sim}{H}_A$ is along the Z axis of the laboratory axis system (XYZ). $\underset{\sim}{E}_{\parallel}$ is parallel to $\underset{\sim}{H}_A$, and $\underset{\sim}{E}_{\perp}$ is perpendicular to $\underset{\sim}{H}_A$. β is the angle between the normal to the membrane $\hat{n}$ ($\hat{n}$ is also the z axis of the molecular axis system) and the hypothetical normal to a perfect cylinder $\hat{N}$.

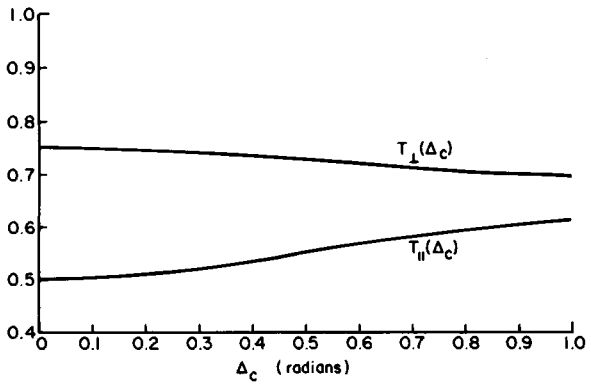

FIGURE 10 $T_\parallel(\Delta_C)$ and $T_\perp(\Delta_C)$ for *Rps. viridis* and *Rps. palustris* in a magnetic field.

complicated by the morphology; briefly, using the coordinate system shown in Fig. 9, we found that a four-rotation scheme *ZXYZ* (angles α, β, γ, and χ) with weighting function $w_C = \exp(-\beta^2/\Delta_C^2)$ will generate this ensemble (see reference 5 or 7 for details). The first two rotations locate the molecular axis system with respect to the cylindrical membranes, and the last two rotations locate the cylinder with respect to the laboratory axis system. Note that the last two free rotations require that the cylinder be perpendicular to the alignment field. The density of states for $\underset{\sim}{E}_\parallel$ along the alignment field and $\underset{\sim}{E}_\perp$ perpendicular to the alignment field are

$$D_\parallel(\theta, \Delta_C) = D_{3,90}^{ZXYZ}[\theta, w_C] \tag{41}$$

and

$$D_\perp(\theta, \Delta_C) = D_{2,0}^{ZXYZ}[\theta, w_C]. \tag{42}$$

$T_\parallel(\Delta_C)$ and $T_\perp(\Delta_C)$ are plotted in Fig. 10.

In reference 7, we used $D_\parallel(\theta, \Delta_C)$ and $D_\perp(\theta, \Delta_C)$ to simulate the EPR spectra of the triplet state of the primary electron donors in both *Rps. viridis* and *Rps. palustris*. We were able to calculate the orientation of the principal magnetic axes with respect to the membrane normal. As a byproduct of our calculation, we found that Δ_{RV} and Δ_P are restricted to small regions:

$$0.3 \text{ rad} \leq \Delta_{RV} \leq 0.5 \text{ rad} \tag{43}$$

and

$$0.4 \text{ rad} \leq \Delta_P \leq 0.6 \text{ rad}. \tag{44}$$

We can now use this information for linear dichroism calculations on the same systems.

Rps. viridis Linear Dichroism

The long wavelength absorption maximum in whole cells of *Rps. viridis* is due to antenna BChl *b* molecules. Because these molecules do not all have the same orientation with respect to the membrane normal, the long wavelength absorption does not correspond to a single molecular species with a unique orientation. This problem can be circumvented by treating

absorption changes induced by unpolarized light and measuring $\Delta A_{\parallel}$ and $\Delta A_{\perp}$ with light polarized parallel and perpendicular to the alignment field, respectively. For light-induced absorption changes, there is a pure transition at 970 nm due to the oxidation of the reaction center BChl *b* dimer P970, which functions as the primary electron donor in *Rps. viridis* (24). Lastly, we note that the same formulas that apply to R and L in the Theory section also apply to ΔR and ΔL defined using $\Delta A_{\parallel}$ and $\Delta A_{\perp}$.

Paillotin et al. (13) have measured the absorption change linear dichroism of magnetically aligned whole cells of *Rps. viridis* and found $\Delta L = -0.42$ at 970 nm. From Eq. 23 and the limits of Δ_{RV} in Eq. 42, ΔL cannot be < -0.33, which results in a discrepancy with experiment. There are two possible explanations: (*a*) The EPR experiments of Frank et al. (7) where Δ_{RV} was determined were done under experimental conditions different from those of the linear dichroism experiments, which may affect Δ_{RV}. (*b*) Perhaps the cell morphology is not adequately defined by our model.

The large negative value for ΔL indicates that ϵ is probably close to 90°. The ideal experiment to do next is magnetophotoselection (25) on P970; this experiment combined with the results in reference 7 would yield an independent value of ϵ.

Rps. palustris Linear Dichroism

The only linear dichroism measurements reported for *Rps. palustris* have been in direct absorption (26, 27). Although there are no isolated transitions due to a single molecular species with a fixed orientation with respect to the membrane normal, we will analyze the three absorption bands at 590, 800, and 870 nm and interpret the results as an average orientation of the transition moments contributing to those peaks.

At 590, 800, and 870 nm, Breton measured dichroic ratios in magnetically aligned *Rps. palustris* of 0.59, 0.81, and 0.80, respectively (26). From $T_{\parallel}(\Delta_P)$ and $T_{\perp}(\Delta_P)$ in Fig. 10, Eq. 19, and the range for Δ_P, we find the following limits on the average angles:

$$0 < \langle \epsilon_{590} \rangle < 20°, \tag{45}$$

$$72° < \langle \epsilon_{800} \rangle < 81°, \tag{46}$$

and

$$71° < \langle \epsilon_{870} \rangle < 78°. \tag{47}$$

In the next section, we use these ranges to investigate the orientation of *Rps. palustris* in a flow method.

Rps. palustris in a Flow System

Morita and Miyazaki (27) have measured the linear dichroism of *Rps. palustris* oriented by a velocity gradient created in a flow system. In a flow system, rod-like particles such as *Rps. palustris* tend to orient such that the long axis of the rod is along a line of constant velocity of the flowing solvent (28). Because the flow system of Morita and Miyazaki (27) has a square cross section perpendicular to the flow direction, any tilt of the long axis away from the flow direction will move the long axis out of a line of constant velocity. We can therefore qualitatively analyze this flow system as a set of cells that tend to orient with the long axis of the cell collinear with the flow direction (Fig. 11). We have not attempted a detailed analysis

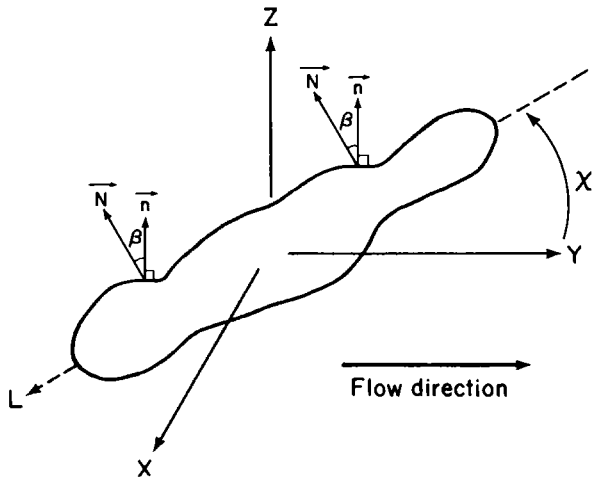

FIGURE 11 Definition of the angles and axis systems for flow-oriented *Rps. palustris*. The flow direction is along the *Y* axis of the laboratory axis system (*XYZ*). $\underset{\sim}{E}_{\parallel}$ is parallel to the flow direction and $\underset{\sim}{E}_{\perp}$ is perpendicular to the flow direction. β is the angle between the membrane normal $\hat{n}$ ($\hat{n}$ is also the *z* axis of the molecular axis system) and the hypothetical normal to a perfect cylinder $\hat{N}$. χ is the angle between the flow direction and the long axis of the cylinder *L*.

of flow orientation; instead, we introduce a Gaussian distribution for the angle between the long axis of the cell and the flow direction χ with width Δ_F

$$w = w(\chi) = \exp(-\chi^2/\Delta_F^2). \tag{48}$$

To generate the flow system ensemble, we begin with the same first two rotations that were used with magnetic field alignment, because these rotations orient the molecular axis system with respect to the hypothetical perfect cylinders, which means they are properties of the cell and not of the alignment method. Note that with the models we are using, Δ_P is unaffected by the alignment method. Three more rotations are necessary to orient the cylinder with respect to the laboratory axis system. The three rotations are: a free rotation of γ about the laboratory *Y* axis; a rotation of χ about the laboratory *X* axis weighted by the Gaussian function in Eq. 48; and a free rotation of ξ about the laboratory *Y* axis. This rotation scheme contains five rotations (*ZXYXY*) which makes the density of states very difficult to evaluate. We note, however, that the fifth rotation is superfluous for the parallel density of states because it is a rotation about $\underset{\sim}{E}_{\parallel}$ (Fig. 11). Thus

$$D_{\parallel}(\theta, \Delta_P, \Delta_F) = D_{3,0}^{ZXYZ}[\theta, w_F],$$

where

$$w_F(\Delta_P, \Delta_F) = \exp(-\beta^2/\Delta_P^2)\exp(-\chi^2/\Delta_F^2).$$

Because the laboratory reference frame is axially symmetric and $\underset{\sim}{E}_{\parallel}$ is along the laboratory symmetry axis, we can calculate $T_{\perp}(\underset{\sim}{\Delta})$ from $T_{\parallel}(\underset{\sim}{\Delta})$ by using Eq. 21, and thus do not need to calculate $D_{\perp}(\theta, \Delta_P, \Delta_F)$.

Morita and Miyazaki (27) measured dichroic ratios of 0.54, 1.27, and 1.26 at 590, 800, and 870 nm, respectively, in flow-oriented *Rps. palustris*. We first set Δ_P to its lower limit of 0.4

rad; this limit corresponds to the limiting values in Eqs. 45–47 of $\langle \epsilon_{590} \rangle = 20°$, $\langle \epsilon_{800} \rangle = 72°$, and $\langle \epsilon_{870} \rangle = 71°$. Working backwards with Eq. 19, we find that $\Delta_F = 0.95$ rad is consistent with these angles. This calculation reveals two important facts. First, because $\Delta_P = 0.4$ is a lower limit, $\Delta_F = 0.95$ rad is an upper limit. Second, the fact that one Δ_F value reproduces all three angles indicates that the models are self-consistent. Analagously, from the $\Delta_P = 0.6$-rad limit, we find a lower limit on Δ_F of 0.90 rad. In summary, the width of the Gaussian distribution in χ, which is a measure of the extent of orientation by flow method, is between 0.90 and 0.95 rad.

DISCUSSION

We have used the density of states formalism to develop a new approach to the theory of linear dichroism. Although equivalent to the Wigner expansion and other similar techniques (3, 4, 13), we find four distinct benefits when adopting the density of states approach.

(*a*) The $\underset{\sim}{\Delta}$ parameters required to represent the distribution function are likely to have greater physical meaning and be fewer in number than the moments of the Wigner expansion. In fact, the moments P_{lmn} could be written in terms of $\underset{\sim}{\Delta}$ by the equation

$$P_{lmn} = \int\int\int \mathcal{D}^{l}_{mn}(\theta', \phi', \psi') F(\theta', \phi', \psi', \underset{\sim}{\Delta})\, d\theta'\, d\phi'\, d\psi', \tag{49}$$

where $F(\theta, \phi', \psi', \underset{\sim}{\Delta})$ is a distribution function which could be derived from $D(\theta, \phi, \underset{\sim}{\Delta})$ by converting from the molecular axis system to the laboratory axis system.

(*b*) Each Δ_i is related to some structural feature of the ordered ensemble and, as such, is a quantity of interest. This is unlike the moments P_{lmn}, which are purely mathematical projections of the Wigner rotation matrix elements on the distribution function. Because $\underset{\sim}{\Delta}$ relates to structural properties of the system, it may be possible to place limits on $\underset{\sim}{\Delta}$ and therefore to place limits on P_{lmn} through Eq. 49. These limits could not be placed directly on P_{lmn}, because there would be no justification for this procedure.

(*c*) There exists a formalism for calculating $D(\theta, \phi, \underset{\sim}{\Delta})$ from arbitrary models (5, 6). Previous attempts by Fraser (8–11) and Beer (12) to interpret linear dichroism have relied on simple models. One such model considers a sample to have a fraction f of the molecules perfectly ordered and the remaining fraction $1 - f$ randomly ordered. The dichroic ratio is then given by

$$R = \frac{2f\cos^2\epsilon + (2/3)(1-f)}{f\sin^2\epsilon + (2/3)(1-f)}. \tag{50}$$

Because this model is probably not realistic, f is a relatively meaningless parameter. In contrast, our $\underset{\sim}{\Delta}$ parameter derived from more realistic models reveals more details about the system. Also, it is straightforward to extend our techniques to include more complicated models. For example, instead of using Gaussian weighting functions, a rotation could be weighted by a potential energy function

$$w(\beta) = \exp\left[-E(\beta, \underset{\sim}{\Delta})/kT\right], \tag{51}$$

where $E(\beta, \Delta)$ is energy as a function of β, k is Boltzmann's constant, and T is temperature. In

principle, several experiments on a system could be used to develop a detailed explanation of the partial ordering.

(*d*) That we average orientations in the molecular axis system instead of the laboratory axis system leads to simplification of the formulas in many instances. When both the laboratory reference frame and the molecular reference frame are axially symmetric, $P(\theta')$ depends only on θ' and $D(\theta, \underline{\Delta})$ depends only on θ. But, when axial symmetry in the laboratory reference frame is lost, $P(\theta', \phi')$ depends on two angles, θ' and ϕ', which are the spherical angles of the molecular reference frame symmetry axis in the laboratory axis system. In contrast, $D(\theta, \underline{\Delta})$ still depends only on θ because it is a distribution function in the axially symmetric molecular reference frame. We can, therefore, consider complex models with nonaxially symmetric laboratory reference frames while still in the realm of axial symmetry. An example is the Elliptical Gaussian Uniaxial Model for which there is no symmetry axis in the laboratory reference frame; we were still able to use an axially symmetric analysis. When all axial symmetry is lost, $P(\theta', \phi', \psi')$ depends on all three angles; but $D(\theta, \phi, \underline{\Delta})$ never depends on more than two angles, because it takes only two angles to specify the orientation of the polarized field in the molecular axis system. Thus, by working in an axis system fixed with respect to the transition moment, we gain computational efficiency.

APPENDIX A

In reference 6, we give some simple formulas and techniques for calculating density of states functions. A brief summary of that approach is given here. The notation for a density of states is

$$D^{RS}_{\upsilon,\psi}[\theta, \phi, w], \tag{A-1}$$

where RS is the rotation scheme (i.e., the number and order of rotations required to generate the ensemble of molecular axis systems), υ is the type of field vector [$\upsilon = 1$ for $E = (\cos\psi, \sin\psi, 0)$, $\upsilon = 2$ for $E = (\cos\psi, 0, \sin\psi)$, and $\upsilon = 3$ for $E = (0, \cos\psi, \sin\psi)$], ψ is the angle in the type of field vector indicated by υ, θ and ϕ are the spherical angles of the field vector in the molecular axis system, and w is the weighting function. Note that $D^{RS}_{\upsilon,\psi}[\theta, \phi, w]$ is a function of the weighting function w; that is, $D^{RS}_{\upsilon,\psi}[\theta, \phi, w]$ is a functional, which we denote with square brackets.

When one is faced with a density of states calculation, the procedure is as follows: (*a*) determine RS, the number and order of rotations required to generate the ensemble; (*b*) determine $w(\alpha\beta\gamma\ldots)$, the product of the weighting functions; and (*c*) determine υ and ψ for the field vector. The formulas for rotation schemes with three or four rotations are given in reference 6.

APPENDIX B

Linear dichroism is reported in a variety of forms. Here, we will relate several of those forms to $R = A_\parallel/A_\perp$ or $L = (A_\parallel - A_\perp)/A$, which we have used in this paper.

After separate measurements of $A_\parallel$ and $A_\perp$, the following four definitions of linear dichroism are sometimes found

$$LD_1 = \frac{A_\parallel - A_\perp}{A_\parallel + A_\perp} = \frac{R - 1}{R + 1} \tag{B-1}$$

$$LD_2 = \frac{A_\parallel - A_\perp}{A_\parallel + 2A_\perp} = \frac{R - 1}{R + 2} \tag{B-2}$$

$$LD_3 = \frac{A_\parallel - A_\perp}{\frac{1}{2}(A_\parallel + A_\perp)} = \frac{2(R-1)}{R+1} \tag{B-3}$$

$$LD_4 = \frac{A_\parallel - A_\perp}{\frac{1}{3}(A_\parallel + 2A_\perp)} = \frac{3(R-1)}{R+2}. \tag{B-4}$$

The dichroic ratio R is related to these four forms by

$$R = \frac{1 + LD_1}{1 - LD_1} \tag{B-5}$$

$$R = \frac{1 + 2LD_2}{1 - LD_2} \tag{B-6}$$

$$R = \frac{2 + LD_3}{2 - LD_3} \tag{B-7}$$

$$R = \frac{3 + 2LD_4}{3 - LD_4}. \tag{B-8}$$

Alternatively, $A_\parallel - A_\perp$ can be measured by lock-in techniques (14–16) and normalized by dividing by A_r or A_{unpol}, which is the absorbance of the oriented sample using unpolarized light. We have already discussed normalization of $A_\parallel - A_\perp$ by A_r, which gives L. A_{unpol} can be written in terms of $A_\parallel$ and $A_\perp$. Following Zbindin, (2)

$$A_\chi = A_\parallel \cos^2 \chi + A_\perp \sin^2 \chi, \tag{B-9}$$

where A_χ is absorbance due to a field $\underset{\sim}{E}_\chi$ whose polarization makes an angle χ with $\underset{\sim}{E}_\parallel$. Integrating over χ, we find

$$A_{\text{unpol}} = \tfrac{1}{2}(A_\parallel + A_\perp). \tag{B-10}$$

Therefore

$$\frac{A_\parallel - A_\perp}{A_{\text{unpol}}} = \frac{A_\parallel - A_\perp}{\frac{1}{2}(A_\parallel + A_\perp)} = LD_3, \tag{B-11}$$

and we can relate this form to R by Eq. B-7.

This work was supported, in part, by the Biomedical and Environmental Research Division of the U.S. Department of Energy under contract No. 2-7405-ENG-48 and, in part, by National Science Foundation grant PCM 76-5074. J. A. Nairn was supported by a University of California Regents Fellowship, and Dr. Frank was supported by a postdoctoral fellowship from the National Institutes of Health.

Received for publication 20 August 1979 and in revised form 27 May 1980.

REFERENCES

1. HOFRICHTER, J., and W. A. EATON. 1976. Linear dichroism of biological chromophores. *Annu. Rev. Biophys. Bioeng.* 5:511–560.

2. ZBINDEN, R. 1964. Infrared Spectroscopy of High Polymers. Academic Press, Inc., New York. 166–233.
3. MCBRIERTY, V. J. 1974. Use of rotation operators in the general description of polymer properties. *J. Chem. Phys.* **61**:872–882.
4. ROTHSCHILD, K. J., and N. A. CLARK. 1979. Polarized infrared spectroscopy of oriented purple membrane. *Biophys. J.* **25**:473–487.
5. FRIESNER, R., J. A. NAIRN, and K. SAUER. 1979. Direct calculation of the orientational distribution function of partially ordered ensembles from the EPR lineshape. *J. Chem. Phys.* **71**:358–365; 5388 (Erratum).
6. FRIESNER, R., J. A. NAIRN, and K. SAUER. 1979. A general theory of the spectroscopic properties of partially ordered ensembles. I. One Vector Problems. *J. Chem. Phys.* **72**:221–230.
7. FRANK, H. A., R. FRIESNER, J. A. NAIRN, G. C. DISMUKES, and K. SAUER. 1979. The orientation of the primary donor in bacterial photosynthesis. *Biochim. Biophys. Acta.* **547**:484–501.
8. FRASER, R. D. B. 1953. The interpretation of infrared dichroism in fibrous protein structures. *J. Chem. Phys.* **21**:1511–1515.
9. FRASER, R. D. B. 1956. Interpretation of infrared dichroism in fibrous proteins. The 2μ region. *J. Chem. Phys.* **24**:89–95.
10. FRASER, R. D. B. 1958. Interpretation of infrared dichroism in axially oriented polymers. *J. Chem. Phys.* **28**:1113–1115.
11. FRASER, R. D. B. 1958. Determination of transition moment orientation in partially oriented polymers. *J. Chem. Phys.* **29**:1428–1429.
12. BEER, M. 1956. Quantitative interpretation of infrared dichroism in partly oriented polymers. *Proc. R. Soc. Lond. Ser. A. Math. Phys. Sci.* **236**:136–140.
13. PAILLOTIN, G., A. VERMEGLIO, and J. BRETON. 1979. Orientation of reaction center and antenna chromophores in the photosynthetic membrane of *Rhodopseudomonas viridis*. *Biochim. Biophys. Acta.* **545**:249–264.
14. CHABAY, I., E. C. HSU, and G. HOLZWARTH. 1972. Infrared circular dichroism measurement between 2000 and 5000 cm^{-1}: Pr^{+3}-tartrate complexes. *Chem. Phys. Lett.* **15**:211–214.
15. GALE, R., A. J. MCCAFFERY, and R. SHATWELL. 1972. Linear dichroism, an adjunct to polarised crystal spectroscopy. *Chem. Phys. Lett.* **17**:416–418.
16. STEIN, R. S. 1961. A procedure for the accurate measurement of infrared dichroism of oriented film. *J. Appl. Polymer Sci.* **5**:96–99.
17. RAFFERTY, C. N., and R. K. CLAYTON. 1979. Linear dichroism and the orientation of reaction centers of *Rhodopseudomonas sphaeroides* in dried gelatin films. *Biochim. Biophys. Acta.* **545**:106–121.
18. RAFFERTY, C. N., and R. K. CLAYTON. 1978. Properties of reaction centers of *Rhodopseudomonas sphaeroides* in dried gelatin films: linear dichroism and low temperature spectra. *Biochim. Biophys. Acta.* **502**:51–60.
19. STRALEY, S. C., W. W. PARSON, D. C. MAUZERALL, and R. K. CLAYTON. 1973. Pigment content and molar extinction coefficients of photochemical reaction centers from *Rhodopseudomonas spheroides*. *Biochim. Biophys. Acta.* **305**:597–609.
20. PARSON, W. W., and R. J. COGDELL. 1975. The primary photochemical reaction of bacterial photosynthesis. *Biochim. Biophys. Acta.* **416**:105–149.
21. GIESBRECHT, P., and G. DREWS. 1966. Über die organisation und die makromolekulare architektur der thylakoide "lebender" bakterien. *Arch. Mikrobiol.* **54**:297–330.
22. TAUSCHEL, H.-D., and G. DREWS. 1967. Thylakoid-morphogenese bei *Rhodopseudomonas palustris*. *Arch. Mikrobiol.* **59**:381–404.
23. GEACINTOV, N. E., F. VAN NOSTRAND, J. F. BECKER, and J. B. TINKEL. 1972. Magnetic field induced orientation of photosynthetic systems. *Biochim. Biophys. Acta.* **267**:65–79.
24. BLANKENSHIP, R. E., and W. W. PARSON. 1979. Kinetics and thermodynamics of electron transfer in bacterial reaction centers. *In* Photosynthesis in Relation to Model Systems. J. Barber, editor. Elsevier/North-Holland Biomedical Press, Amsterdam. 71–114.
25. FRANK H. A., J. BOLT, R. FRIESNER, and K. SAUER. 1979. Magnetophotoselection of the triplet state of reaction centers from *Rhodopseudomonas sphaeroides* R-26. *Biochim. Biophys. Acta.* **547**:502–511.
26. BRETON, J. 1974. The state of chlorophyll and carotenoid in vivo, II. A linear dichroism study of pigment orientation in photosynthetic bacteria. *Biochem. Biophys. Res. Commun.* **59**:1011–1017.
27. MORITA, S., and T. MIYAZAKI. 1971. Dichroism of bacteriochlorophyll in cells of the photosynthetic bacterium *Rhodopseudomonas palustris*. *Biochim. Biophys. Acta.* **245**:151–159.
28. JEFFERY, G. B. 1923. The motion of ellipsoidal particles immersed in a viscous fluid. *Proc. R. Soc. Lond. Ser. A. Math. Phys. Sci.* **102**:161–179.